

An Evaluation of Biofield Treatment on Thermal, Physical and Structural Properties of Cadmium Powder

Mahendra Kumar Trivedi¹, Gopal Nayak¹, Shrikant Patil¹, Rama Mohan Tallapragada¹, Omprakash Latiyal², and Snehasis Jana^{2*}

¹Trivedi Global Inc., 10624 S Eastern Avenue Suite A-969, Henderson, NV 89052, USA

²Trivedi Science Research Laboratory Pvt. Ltd., Hall-A, Chinar Mega Mall, Chinar Fortune City, Hoshangabad Rd., Bhopal- 462026 Madhya Pradesh, India

Abstract

Cadmium is widely utilized in nickel-cadmium batteries, stabilizers, and coating applications due to its versatile physico-chemical properties. The aim of present study was to evaluate the impact of biofield treatment on atomic, thermal, and physical properties of cadmium powder. The cadmium powder was divided into two groups, one group as control and another group as treated. The treated group received Mr. Trivedi's biofield treatment. Control and treated samples were characterized using X-ray diffraction (XRD), differential scanning calorimetry (DSC), particle size analyzer, surface area analyzer, and scanning electron microscopy (SEM). XRD results showed significant alteration in lattice parameter, unit cell volume, densities, nuclear charge per unit volume, and atomic weight in treated cadmium powder as compared to control. Furthermore, crystallite size was significantly reduced upto 66.69% in treated cadmium as compared to control. DSC analysis results showed that the latent heat of fusion of the treated cadmium powder was considerably reduced by 16.45% as compared to control. Particle size data revealed that average particle size (d_{50}) of treated cadmium powder was significantly reduced by 47.79 % as compared to the control. In addition, the surface area of treated cadmium powder was substantially enhanced by 156.36% as compared to control. Surface morphology observed by SEM showed the more facets and fractured surface with satellite boundaries in treated cadmium powder as compared to control. These findings suggest that biofield treatment has significantly altered the atomic, thermal and physical properties of cadmium.

Keywords: Biofield treatment; Cadmium; X-ray diffraction; Differential scanning calorimetry; Particle size; Surface area; Scanning electron microscopy

Introduction

Cadmium (Cd) element belongs to group IIB in the Periodic Table, which originally exists in Hexagonal Closed Packing (HCP) crystal structure. Cadmium is widely used in battery, predominantly in rechargeable nickel-cadmium batteries as anode, stabilizers, coating applications etc. Higher specific surface area of a material plays an important role in many applications including battery electrodes, catalyst supports, and energy storage devices [1]. The increase in surface area of the electrodes in batteries leads to improve the cell current density and thus, deliver more power [2]. Besides that, in industries, high surface area is achieved *via* various methods such as ball milling, and laser-assisted chemical vapour deposition, etc [3-5]. Nevertheless, these processes require complex and expensive methods that can limit the application of these materials. Thus, researchers have investigated alternative ways to increase the surface area. After considering of cadmium properties and cost aspect, the authors wanted to investigate an alternative and economically viable approach that could be beneficial to modify the atomic, structural, and thermal properties of powder. The law of mass-energy inter-conversion has existed in the literature for more than 300 years for which first idea was given by Hasenohrl, after that Einstein derived the well-known equation $E=mc^2$ for light and mass [6,7]. However the conversion of mass into energy is fully verified, but the inverse of this relation, i.e. energy into mass has not yet verified scientifically. Furthermore, the energy exists in various forms such as kinetic, potential, electrical, magnetic, and nuclear, etc. Similarly, human nervous system consists of neurons, which have the ability to transmit information in the form of electrical signals [8-10]. Thus, a human has ability to harness the energy from environment/universe and it can transmit into any object (living or non-living) on the Globe. The object always receives the energy and responded into

useful way and that is called biofield energy. This process is known as biofield treatment. Mr. Trivedi's biofield treatment (The Trivedi effect) has known to transform the characteristics in various fields such as material science [11-14], microbiology [15-17], biotechnology [18,19], and agriculture [20-22]. In metals and ceramics the biofield treatment has shown the excellent results in physical, thermal, and atomic level. In addition, the biofield treatment had increased the particle size by six folds and enhanced the crystallite size by two folds in zinc powder [11]. Based on the outstanding result achieved by biofield treatment on metals and ceramics, an attempt was made to evaluate the effect of biofield treatment on at atomic, thermal and structural properties of cadmium powder.

Experimental

Cadmium powder used in present investigation was procured from Alpha Aesar, USA. The cadmium powder sample was divided into two parts, referred as control and treated. The treated part was received Mr. Trivedi's biofield treatment. Control and treated samples were characterized using X-ray diffraction (XRD), differential scanning calorimetry (DSC), particle size analyzer, surface area analyzer, and scanning electron microscopy (SEM).

*Corresponding author: Snehasis J, Trivedi Science Research Laboratory Pvt. Ltd., Hall-A, Chinar Mega Mall, Chinar Fortune City, Hoshangabad Rd., Bhopal- 462026, Madhya Pradesh, India, Tel: 917556660006; E-mail: publication@trivedisrl.com

Received July 07, 2015; Accepted July 23, 2015; Published August 04, 2015

Citation: Trivedi MK, Nayak G, Patil S, Tallapragada RM, Latiyal O et al. (2015) An Evaluation of Biofield Treatment on Thermal, Physical and Structural Properties of Cadmium Powder. J Thermodyn Catal 6: 147. doi:10.4172/2157-7544.1000147

Copyright: © 2015 Mahendra Kumar T, et al. This is an open-access article distributed under the terms of the Creative Commons Attribution License, which permits unrestricted use, distribution, and reproduction in any medium, provided the original author and source are credited.

X-ray diffraction analysis

XRD analysis of control and treated cadmium powder was performed using Phillips, Holland PW 1710 XRD diffractometer, which had a copper anode with nickel filter. The wavelength of X-ray radiation used was 1.54056 Å. Data obtained from the XRD was in chart form of intensity vs. 2θ°, with a detailed table containing d value (Å), number of peaks, peak width 2θ°, peak count, relative intensity of peaks, etc. Further, lattice parameter and unit cell volume were computed using PowderX software.

$$\text{Crystallite size} = k \lambda / b \cos \theta.$$

Where, λ is the wavelength of x-ray (=1.54056 Å) and k is the equipment constant (=0.94).

Besides, the percent change in the lattice parameter was calculated using following equation:

$$\% \text{ change in lattice parameter} = \frac{[A_{\text{Treated}} - A_{\text{Control}}]}{A_{\text{Control}}} \times 100$$

Where A_{Control} and A_{Treated} are the lattice parameter of treated and control samples respectively. Similarly, the percent change in all other parameters such as unit cell volume, density, atomic weight, nuclear charge per unit volume, crystallite size was calculated. For XRD analysis treated sample was divided into four parts referred as T1, T2, T3 and T4.

Thermal analysis

For thermal analysis, Differential Scanning Calorimeter (DSC) of Perkin Elmer/Pyris-1, USA with a heating rate of 10°C/min and nitrogen flow of 5 ml/min was used. Melting point and latent heat of fusion were obtained from the DSC curve.

Percent change in melting point was calculated using following equations:

$$\% \text{ change in Melting point} = \frac{[T_{\text{Treated}} - T_{\text{Control}}]}{T_{\text{Control}}} \times 100$$

Where, T_{Control} and T_{Treated} are the melting point of control and treated samples, respectively.

Percent change in latent heat of fusion was calculated using following equations:

$$\% \text{ change in Latent heat of fusion} = \frac{[\Delta H_{\text{Treated}} - \Delta H_{\text{Control}}]}{\Delta H_{\text{Control}}} \times 100$$

Where, $\Delta H_{\text{Control}}$ and $\Delta H_{\text{Treated}}$ are the latent heat of fusion of control and treated samples, respectively.

Particle size and surface area analysis

Laser particle size analyzer, Sympatec HELOS-BF was used to

determine the particle size distribution, which had a detection range of 0.1–875 μm. The data obtained from the instrument was in the form of a chart of cumulative percentage vs. particle size. Average particle size d_{50} and d_{99} (size below which 99% particle are present) were computed from particle size distribution curve. Percent change in particle size was calculated using following equations:

$$\% \text{ change in particle size, } d_{50} = \frac{[(d_{50})_{\text{Treated}} - (d_{50})_{\text{Control}}]}{(d_{50})_{\text{Control}}} \times 100$$

Where, $(d_{50})_{\text{Control}}$ and $(d_{50})_{\text{Treated}}$ are the particle size, d_{50} of control and treated samples respectively. Similarly, the percent change in particle size d_{99} was calculated.

The surface area was measured by the Surface area analyser, Smart SORB 90 based on Brunauer-Emmett-Teller (BET), which had a detection range of 0.2–1000 m²/g. Percent change in surface area was calculated using following equations:

$$\% \text{ change in surface area} = \frac{[S_{\text{Treated}} - S_{\text{Control}}]}{S_{\text{Control}}} \times 100$$

Where, S_{Control} and S_{Treated} are the surface area of control and treated samples respectively.

Scanning electron microscopy

Structure and surface morphology are the unique properties of powder. Thus, control and treated cadmium samples were observed using JEOL JSM-6360 SEM instrument at 500X magnification. Differences in the tendency of the particles to aggregate were easily seen at the lower magnifications, while variations in size and morphology become clearer at higher magnification [23].

Results and discussion

X-ray diffraction analysis

XRD analysis results of cadmium powder is illustrated in Table 1 and Figures 1-3. Data showed that the lattice parameter in cadmium was increased by 0.05, 0.20, 0.36 and 0.26% in T1, T2, T3, and T4 sample respectively, as compared to control. This lead to increase the unit cell volume by 0.10, 0.41, 0.73, and 0.53% in T1, T2, T3, and T4 sample respectively, as compared to control. Moreover, this increase in unit cell volume led to reduce the density by 0.10, 0.41, 0.72 and 0.53% in T1, T2, T3, and T4 respectively, as compared to control. Thus, the increased in unit cell volume and decreased in density in treated cadmium indicates that tensile stress may be applied through biofield treatment on cadmium powder [24]. Sirdeshmukh et al. reported that lattice strain was generated in cadmium-telluride powder after grinding and milling the powder for different durations [25]. Hence, it is assumed that an energy milling might be induced through biofield treatment, which probably provided the high stress and that might be responsible for internal strain in treated cadmium. Furthermore, the atomic weight was increased in cadmium powder by 0.10, 0.41, 0.73 and 0.53 % in

Group	Lattice Parameter (Å)	Unit Cell Volume ($\times 10^{-23}$ cm ³)	Density (g/cc)	Atomic Weight (g/mol)	Nuclear charge per unit volume (C/cm ³)	Crystallite Size (nm)
Control	2.979	4.314	8.695	112.96	554458	143.41
T1	2.980	4.319	8.685	113.08	553573	143.39
T2	2.985	4.332	8.659	113.43	551044	86.03
T3	2.990	4.346	8.631	113.79	548403	47.77
T4	2.987	4.337	8.648	113.57	550035	143.33

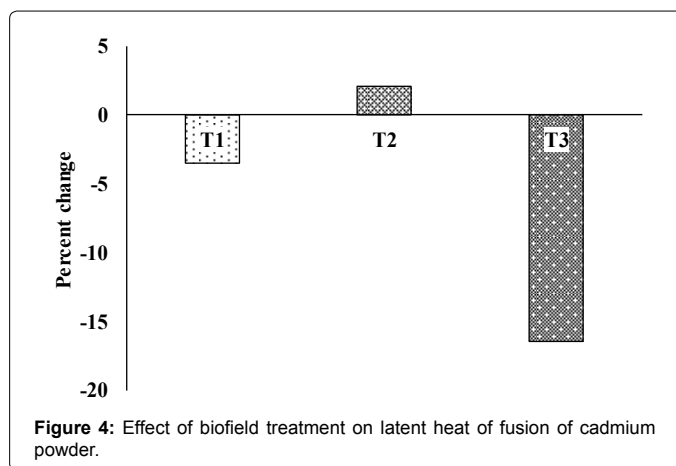
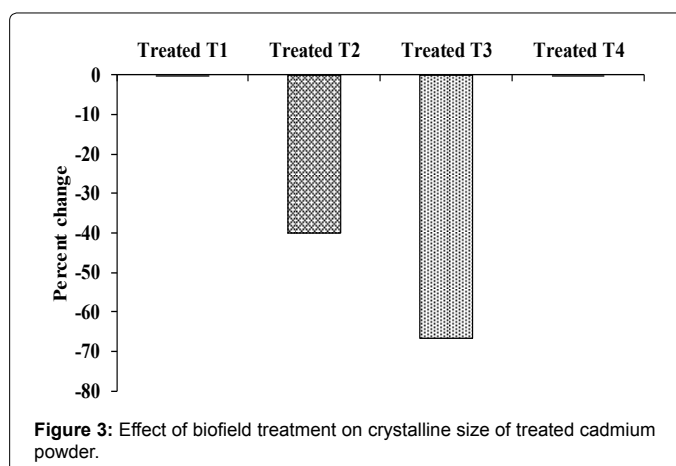
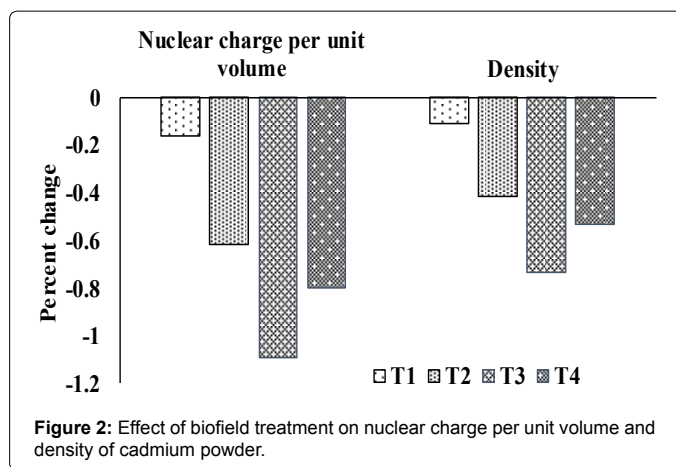
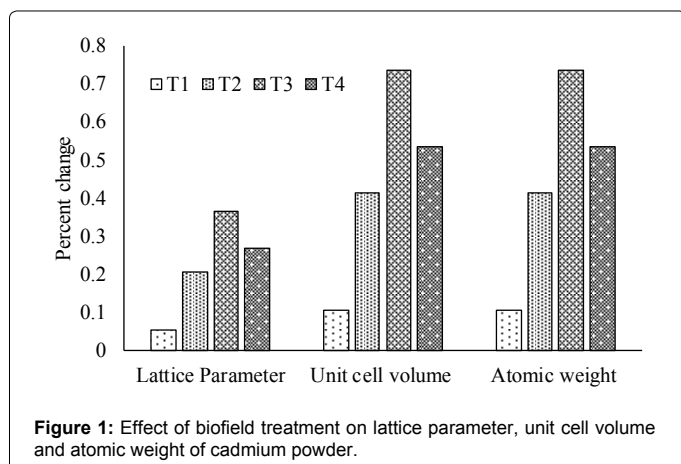
T1, T2, T3 and T4: Treated group

Table 1: X-ray diffraction analysis of cadmium powder.

T1, T2, T3, and T4 respectively, as compared to control (Figure 1). Besides, nuclear charge per unit volume was decreased by 0.15, 0.61, -1.09, and 0.79% in T1, T2, T3, and T4 respectively, as compared to control (Figure 2). It is possible that the tensile stress induced through energy milling over unit cell may lead to move away the electron cloud from their original position [26]. This may be resulted into increase in atomic size (volume of the atom) and reduced nuclear charge per unit volume in treated cadmium. On the other hand, the increased atomic weight and decreased nuclear charge per unit volume suggest that the proton to neutron ratio may alter in treated cadmium powder. Thus, it is postulated that a weak reversible reaction may be induced through biofield treatment, which includes proton-neutron and neutrinos and that possibly resultant into alteration of neutron to proton ratio [24]. In addition, the crystallite size was changed from 143.41 nm (control) to 143.39, 86.03, 47.77, and 143.22nm in T1, T2, T3, and T4 samples, respectively (Figure 3). It indicates that no significant change in crystallite size was found in T1 and T4 sample, but it was significantly reduced in T2 and T3 sample by 50.01 and 66.69% respectively, as compared to control. It is hypothesized that high volumetric strain observed in cadmium unit cell which may deformed the crystallite, which further led to subgrain formation and reduced crystallite size. Thus, XRD data revealed that biofield treatment has significantly changed the atomic and structural properties of cadmium powder.

Thermal analysis

Differential scanning calorimetry (DSC) was used to determine the latent heat of fusion and melting point in cadmium samples, and the results are presented in Table 2 and Figure 4. In a solid, substantial amount of interaction force exists in atomic bonds to hold the atoms at their positions. Latent heat of fusion is defined as the energy required to overcome this interaction force to change the phase and it is stored as potential energy of atoms. However, melting point is related to kinetic energy of the atoms [27]. Based on the XRD result, DSC was carried out for control, T1, T2 and T3 samples. Data showed that latent heat of fusion was changed from 48.8 J/g (control) to 47.08, 49.81, and 40.77 J/g in T1, T2, and T3 sample respectively, as compared to control. It indicates that latent heat of fusion was decreased by 3.5 and 16.45% in T1 and T3 sample, respectively as compared to control. On the contrary the latent heat of fusion was slightly increased by 2.06 % in treated T2 as compared to control (Figure 4). Our group has previously reported that biofield treatment has reduced the latent heat of fusion in lead powder [28]. The reduction of latent heat of fusion after biofield treatment indicates that treated cadmium sample might have some



extra potential energy as compared to control. Thus, it is postulated that, biofield treatment might have transferred energy to cadmium powder, which stored as potential energy of atoms. Due to the presence of extra potential energy in treated cadmium atoms, it may require less (as compared to control) amount of heat to change the phase from solid to liquid and reduced latent heat of fusion. Furthermore, data showed that melting point of cadmium was 322.22, 323.07, 322.39, and 322.74°C in control, T1, T2, and T3 respectively. This data suggest that

Group	Latent Heat of fusion ΔH (J/g)	Melting Point (°C)
Control	48.8	322.22
T1	47.08	323.07
T2	49.81	322.39
T3	40.77	322.74

T1, T2, T3: Treated group

Table 2: Thermal properties of cadmium powder.

Group	d_{50} (μm)	d_{99} (μm)	Surface area (m^2/g)
Control	70.3	204.7	0.05
Treated T1	36.7	121.3	0.13

Table 3: Particle size and surface area of cadmium powder.

no significant change was found in melting point of treated cadmium powder, as compared to control. It indicates that the thermal vibrations and kinetic energy of the atoms may not be affected through biofield treatment. Therefore, it is expected that energy transferred through biofield treatment probably stored as potential energy rather than kinetic energy in treated cadmium powder. Hence, DSC data suggest that biofield treatment has altered the thermal properties of cadmium powder.

Particle size and surface area analysis

Particle size and surface area result of cadmium powder powder are presented in Table 3 and Figure 5. Data showed that the average particle size, d_{50} was significantly reduced from 70.3 μm (control) to 36.7 μm in treated cadmium powder. Particle size, d_{99} was reduced from 204.7 μm (control) to 121.3 μm . It indicates that d_{50} and d_{99} were reduced by 47.79 and 40.7% respectively in treated cadmium powder as compared to control. This could be due to fragmentation of larger particles into smaller particles. However, in order to break the particles, a sufficient amount of stress energy is required that depends upon the size of the particles *i.e.* the smaller the particles, larger the energy needed [29,30]. Thus, it is assumed that this required stress energy might be provided to cadmium particles during energy milling through biofield treatment [31]. Moreover, the significant decrease in particles size of treated cadmium powder possibly resulted in an increase in surface area by 156.36% as compared to control. Similar results of particle size reduction in titanium and antimony had been reported by our group in previous studies [11,12]. Moreover, in nickel-cadmium batteries, cadmium is used as negative electrode plate, which oxidised and release electrons during discharging, thus reduction in particle size of cadmium powder after biofield treatment may increase the specific energy of batteries [32, 33] Furthermore, Iden et al reported that increase in surface area improves the kinetics of electrochemical reactions in batteries [34]. Thus, it is assumed that biofield treated cadmium could be more useful in electrochemical application as compared to control.

Scanning electron microscopy

Figure 6 shows the SEM micrographs of control and treated cadmium powder. The micrograph showed spherical shaped particles in control and treated cadmium powder. Particles were in the size range of 1–40 μm and 1–30 μm in control and treated cadmium powder, respectively. It indicates that coarse cadmium particles might be breakdown into finer and that led to reduced particle size. Besides, large number of facets were observed over the surface of treated cadmium particles, as compared to control. It could be due to energy milling through biofield treatment. In addition, satellite boundaries

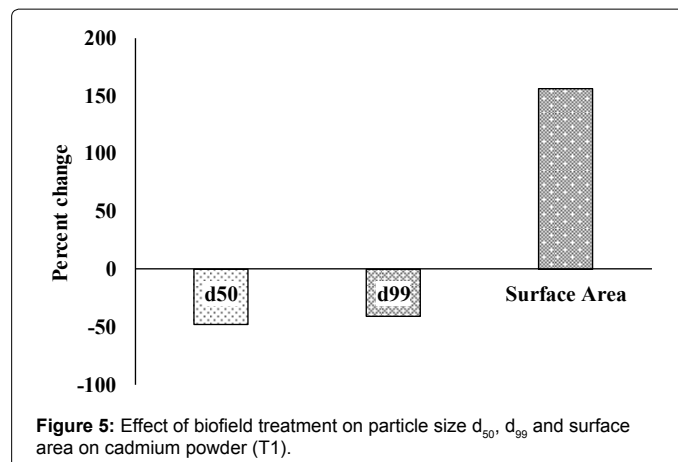


Figure 5: Effect of biofield treatment on particle size d_{50} , d_{99} and surface area on cadmium powder (T1).

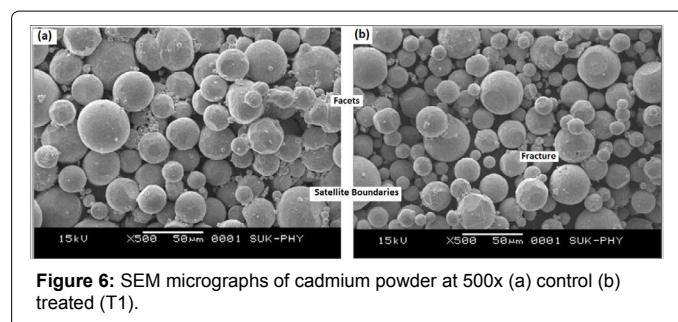


Figure 6: SEM micrographs of cadmium powder at 500x (a) control (b) treated (T1).

were observed in control and treated cadmium powder and fractured surface were found after biofield treatment.

Conclusion

In summary, XRD results showed that crystallite size was decreased by 66.69% in treated cadmium as compared to control that might be due to subgrain formation inside the crystallites through high internal strain. Thermal analysis data revealed that the latent heat of fusion was reduced by 16.45% in treated cadmium as compared to control. It is hypothesized that energy might be transferred through biofield treatment to cadmium atoms and stored in metal as potential energy. Thus, higher potential energy in treated cadmium led to reduced latent heat of fusion. Besides, average particle size was significantly reduced in treated cadmium by 47.7%, as compared to control, which resulted into increase surface area upto 156.36 % after biofield treatment. Moreover, the cadmium with smaller particle size, and high surface area in electrode could improve the kinetics of electrochemical reactions. Therefore it is assumed that biofield treated cadmium could be more useful in nickel-cadmium batteries in electrochemical industries.

Acknowledgement

The authors gratefully acknowledge to Dr. Cheng Dong of NLSC, Institute of Physics and Chinese academy of sciences for providing the facilities to use PowderX software for analyzing XRD results.

The generous support of Trivedi Science, Trivedi Master Wellness and Trivedi Testimonials is gratefully acknowledged.

References

1. Royston E, Ghosh A, Kofinas P, Harris MT, Culver JN, et al. (2008) Self-assembly of virus-structured high surface area nanomaterials and their application as battery electrodes. Langmuir 24: 906-912.
2. Katerina E (2010) High energy density lithium batteries: materials, engineering, applications (1stedn.) John Wiley & Sons.

3. Purushotham E (2015) X-ray Study of measured thermal properties of ball milled Metal Nanopowder. *J Adv Phys* 3: 315-318.
4. Sindhura KS, Prasad TNVKV, Selvam PP, Hussain OM (2015) Green synthesis of zinc nanoparticles from *Senna auriculata* and influence on peanut pot-culture. *IJRAS* 2: 61-69.
5. Guan YF, Pedraza AJ (2008) Synthesis and alignment of Zn and ZnO nanoparticles by laser-assisted chemical vapor deposition. *Nanotechnology* 19: 045609.
6. Hasenohr F (1904) On the theory of radiation in moving bodies. *Annalen der Physik* 15: 344-370.
7. Einstein A (1905) Does the inertia of a body depend upon its energy-content. *Annalen der Physik* 18: 639-641.
8. Becker RO, Selden G (1985) *The body electric: Electromagnetism and the foundation of life (1stedn.)* William Morrow and Company, New York City.
9. Barnes RB (1963) Thermography of the human body. *Science* 140: 870-877.
10. Born M (1971) *The Born-Einstein Letters (1stedn.)* Walker and Company, New York.
11. Trivedi MK, Tallapragada RM (2008) A transcendental to changing metal powder characteristics. *Met Powder Rep* 63: 22-28, 31.
12. Dhabade VV, Tallapragada RM, Trivedi MK (2009) Effect of external energy on atomic, crystalline and powder characteristics of antimony and bismuth powders. *Bull Mater Sci* 32: 471-479.
13. Trivedi MK, Patil S, Tallapragada RM (2012) Thought intervention through bio field changing metal powder characteristics experiments on powder characteristics at a PM plant. *Future Control and Automation* 173: 247-252.
14. Trivedi MK, Patil S, Tallapragada RM (2015) Effect of biofield treatment on the physical and thermal characteristics of aluminium powders. *Ind Eng Manage* 4: 151.
15. Trivedi MK, Patil S, Bhardwaj Y (2008) Impact of an external energy on *Staphylococcus epidermis* [ATCC 13518] in relation to antibiotic susceptibility and biochemical reactions – An experimental study. *J Accord Integr Med* 4: 230-235.
16. Trivedi MK, Patil S (2008) Impact of an external energy on *Yersinia enterocolitica* [ATCC –23715] in relation to antibiotic susceptibility and biochemical reactions: An experimental study. *Internet J Alternat Med* 6.
17. Trivedi MK, Patil S, Bhardwaj Y (2009) Impact of an external energy on *Enterococcus faecalis* [ATCC – 51299] in relation to antibiotic susceptibility and biochemical reactions – An experimental study. *J Accord Integr Med* 5: 119-130.
18. Patil S, Nayak GB, Barve SS, Tembe RP, Khan RR, et al. (2012) Impact of biofield treatment on growth and anatomical characteristics of *Pogostemon cablin* (Benth). *Biotechnology* 11: 154-162.
19. Altekar N, Nayak G (2015) Effect of biofield treatment on plant growth and adaptation. *J Environ Health Sci* 1: 1-9.
20. Shinde V, Sances F, Patil S, Spence A (2012) Impact of biofield treatment on growth and yield of lettuce and tomato. *Aust J Basic Appl Sci* 6: 100-105.
21. Lenssen AW (2013) Biofield and fungicide seed treatment influences on soybean productivity, seed quality and weed community. *Agricultural Journal* 8: 138-143.
22. Sances F, Flora E, Patil S, Spence A, Shinde V, et al. (2013) Impact of biofield treatment on ginseng and organic blueberry yield. *Agrivita J Agric Sci* 35.
23. Dercz G, Prusik K, Pajak L (2008) X-ray and SEM studies on zirconia powders. *JAMME* 31: 408-414.
24. Trivedi MK, Patil S, Tallapragada RM (2013) Effect of biofield treatment on the physical and thermal characteristics of vanadium pentoxide powder. *J Material Sci Eng S11*: 001.
25. Sirdeshmukh DB, Subhadra KG, Hussain KA, Krishna NG, Rao BR, et al. (1993) X-ray study of strained CdTe powders. *Cryst Res Technol* 28: 15-18.
26. Trivedi MK, Tallapragada RM (2009) Effect of superconsciousness external energy on atomic, crystalline and powder characteristics of carbon allotrope powders. *Mater Res Innov* 13: 473-480.
27. Moore WJ (2010) *Chemistry: The molecular science (4thedn.)* Brooks Cole.
28. Trivedi MK, Patil S, Tallapragada RM (2013) Effect of biofield treatment on the physical and thermal characteristics of silicon, tin and lead powders. *J Material Sci Eng* 2: 125.
29. Ohenoja K (2014) Particle size distribution and suspension stability in aqueous submicron grinding of CaCO₃ and TiO₂. Master Thesis, University of Oulu Finland.
30. Schilde C, Breitung-Faes S, Kwade A (2007) Dispersing and grinding of alumina nano particles by different stress mechanisms. *CFI-Ceram Forum Int* 84: 12-17.
31. Trivedi MK, Patil S, Tallapragada RM (2014) Atomic, crystalline and powder characteristics of treated zirconia and silica powders. *J Material Sci Eng* 3: 144.
32. Grugeon S, Laruelle S, Herrera-Urbina R, Dupont L, Poizot P, et al. (2001) Particle Size Effects on the Electrochemical Performance of Copper Oxides toward Lithium. *J Electrochem Soc* 148: A285-A292.
33. Du W, Gupta A, Zhang X, Sastry AM, Shyy W, et al. (2010) Effect of cycling rate, particle size and transport properties on lithium-ion cathode performance. *Int J of Heat & Mass Transf* 53: 3552-3561.
34. Iden H, and Kucernak AR (2014) Analysis of effective surface area for electrochemical reaction derived from mass transport property. *J Electroanal Chem* 734: 61-69.